Synthesis and physico-chemical characterization of fluoride (F)- and silver (Ag)-substituted sol-gel mesoporous bioactive glasses

Research Article

Saeid Kargozar*, Francesco Baino*, Sara Banijamali, and Masoud Mozafari*

Synthesis and physico-chemical characterization of fluoride (F)- and silver (Ag)-substituted sol-gel mesoporous bioactive glasses

https://doi.org/10.1515/bglass-2019-0015
Received Aug 25, 2019; revised Dec 06, 2019; accepted Dec 06, 2019

Abstract: Synthesis and use of novel compositions of bioactive glasses (BGs) for hard tissue engineering are of important significance in the biomedical field. In this study, we successfully synthesized a series of 58S-based BGs containing fluoride (F^-) and silver (Ag^+) ions through a sol-gel method for possible use in bone/dental regeneration and antibacterial strategies. Characterizations of samples were performed by using thermal analyses (thermogravimetric analysis (TGA) and differential scanning calorimetry (DSC)), X-ray diffraction (XRD), Fourier-transform infrared spectroscopy (FTIR), textural analysis (N_2 adsorption-desorption), and morphological observations by transmission electron microscopy (TEM) and scanning electron microscopy (SEM). The obtained data revealed that the fabricated BGs are in a glassy state before incubation in the Kokubo's simulated body fluid (SBF), and an apatite-like layer is formed on their surface after 7 days of immersion in SBF. The size of the glass particles was in the nano-range (about 100 nm or below), and their pore size was in the mesoporous range (15-25 nm). These early results suggest that the F- and Ag-doped glasses show promise as multifunctional bioactive materials for bone/dental tissue engineering.

Keywords: Bioactive glass; Sol-gel; Fluoride; Silver; Bone tissue engineering

1 Introduction

Skeletal disorders are still identified as the most common injuries of the human body. Moreover, the rate of bone defects and diseases are growing so that it will be expected to double by 2020 [1]. Therefore, many attempts have been made worldwide to provide appropriate substitutes for the replacement of damaged bone tissues [2–4]. Although the transplantation of naturally derived grafts, including auto-, allo-, and xenografts, have been commonly applied as the first option, however, the use of synthetic materials has become increasingly important. The reason is associated with the inherent limitations of transplant materials including donor limitation (and hence limited availability), immunogenicity and risk of disease transmission, and ethical issues [5].

Bioactive glasses (BGs) are identified as highly-suitable synthetic bone substitutes due to their excellent characteristics, including osteoinductivity, osteoconductivity, stimulation of angiogenesis, and biocompatibility [6–10]. Today, this type of biomaterials with different compositions is commonly used in clinics for hard and soft tissue repair and regeneration [11–13]. The composition of the first developed BG (45S5 Bioglass) consisted of a silicate quaternary system (45% SiO_2, 24.5% CaO, 24.5% Na_2O, and 6.0% P_2O_5, wt.%) which was invented by Hench in 1969 [14]. Since then, several other chemical formulations of BGs were designed and produced in the shape of powder, granules, and three dimensional (3D) scaffolds for the repair and regeneration of the human tissues [15–17]. Over time, the sol-gel approach has been proposed for the synthesis of porous BGs, in which higher surface reactivity and degradability of glasses are achieved due to the presence of an ultrahigh specific sur-

***Corresponding Author: Saeid Kargozar:** Tissue Engineering Research Group (TERG), Department of Anatomy and Cell Biology, School of Medicine, Mashhad University of Medical Sciences, Mashhad, Iran; Email: kargozarsaeid@gmail.com
***Corresponding Author: Francesco Baino:** Institute of Materials Physics and Engineering, Applied Science and Technology Department, Politecnico di Torino, Corso Duca degli Abruzzi 24, 101 29 Torino, Italy;
Email: francesco.baino@polito.it
***Corresponding Author: Masoud Mozafari:** Cellular and Molecular Research Center, Iran University of Medical Sciences, Tehran, Iran; Department of Tissue Engineering & Regenerative Medicine, Faculty of Advanced Technologies in Medicine, Iran University of Medical Sciences (IUMS), Tehran, Iran; Email: mozafari.masoud@gmail.com
Sara Banijamali: Engineering Ceramics Research Group, Ceramic Department, Materials and Energy Research Center (MERC), P.O. Box: 4777-14155, Tehran, Iran

Table 1: The composition of the synthesized BG samples (mol.%)

Sample	SiO_2	P_2O_5	CaO	CaF_2	Ag_2O
Control (58S BG)	60	4	36	0	0
$5CaF_2/0Ag_2O$	57	3.8	34.2	5	0
$5CaF_2/1Ag_2O$	56.4	3.76	33.84	5	1

face area (>100 m^2/g) associated to the inherent mesoporous texture [18, 19].

In order to improve the biological effects of BGs, the incorporation of various therapeutic ions into the glass structure has been proposed. On this matter, a number of elements such as silver, fluorine, strontium, copper, and cobalt were added to the BGs [20–23]. Each of these ions, once released from the glass structure into the surrounding biological environment, can activate specific genes and pathways for cells and tissues to achieve a desired therapeutic response [24].

In order to enhance bone density and bone mass, fluoride ions (F^-) were added to the structure of BGs in different systems. Fluorine is an inorganic element that plays a significant role in bone and tooth. It has been shown that F^- ions can increase trabecular thickness and bone density, which may be favorable for the treatment of osteoporosis [25, 26]. Moreover, this ion can inhibit the progress of dental cavities due to forming fluorapatite (FAp), which is more acid-resistant than hydroxyapatite (HA) in acidic conditions (*e.g.* in the mouth) [27]. Accordingly, incorporating fluoride ions into BGs and glass-ceramics is of great interest for developing dental as well as orthopedic biomaterials.

Since post-surgical bacterial infections are recognized as one of the main constraints on the way of bone repair, much attention has been made in controlling and preventing bacteria growth and reproduction [28]. In this regard, the incorporation of antibacterial elements like silver [29], copper [30], and zinc [31] into BGs has been proposed as an appropriate approach to inhibit bacterial activities. In a previous work, we synthesized 58S-based BGs co-doped with silver and fluoride ions and tested their antimicrobial activity against bacteria isolated from infected burn wounds of human patients. Specifically, it was shown that the effectiveness of released Ag^+ ions against bacteria and the cytotoxic effect follow a concentration-dependent manner [32]. These early biological results were used as an eliminatory criterion to select the most promising BGs deserving further physico-chemical investigations, which are reported in the present work. These BGs can be considered potentially suitable for application in bone regeneration strategies: to the best of our knowledge, it is the first time that silver and fluoride ions are simultaneously incorporated into the structure of BGs to achieve a dual therapeutic effect, *i.e.* improving osteogenesis and antibacterial activities.

2 Materials and methods

2.1 Synthesis of glass particles

Glass nanopowders containing Ag^+ and F^- ions were synthesized based on 58S BG composition (Table 1) via sol-gel method. Briefly, 14.8 g of tetraethyl orthosilicate (TEOS) was added into 30 mL of 2 M nitric acid solution, and the mixture was allowed to react for 60 min for the acid hydrolysis of TEOS to proceed almost to completion. Then, triethyl phosphate, calcium nitrate tetrahydrate, calcium fluoride (CaF_2) and silver nitrate ($AgNO_3$) were added to the solution, respectively, in appropriate amounts. Next, mixing was continued for 1 h to allow the completion of the reactions. The aging procedure on the prepared sol was performed using incubation at room temperature for 7 days. The resulted gel was heated at 120°C for 24 h, and final calcination at 700°C for 1h was carried out to eliminate nitrates as well as to stabilize and partially densify the glass structure. The prepared BGs were milled and sieved to obtain glass particles with a size below 38 μm. Then, the material was milled again to obtain fine glass particles by high-energy ball milling (Fritsch's planetary ball mill P7).

2.2 Physico-chemical characterization

2.2.1 Thermal analyses

Thermogravimetric analysis (TGA) and differential scanning calorimetry (DSC) were employed to evaluate the thermal behavior of the synthesized glasses. To obtain TGA curves, the samples were analyzed using a Shimadzu TGA-50 device under a nitrogen atmosphere at a heating rate of 5°C/min up to a temperature of 1200°C. In order to determine the crystallization temperatures by DSC, the samples in gel form were introduced into a Shimadzu DSC-50 ana-

lyzer and subjected to a thermal cycle up to 1000°C with a constant heating rate of 10°C min^{-1}.

2.2.2 Densitometry

The density of all the glasses was measured in accordance with Archimedes' principle using analytical balance density determination kits (Thermo-Fisher, USA). The following formula was applied to calculate the density of the prepared glasses:

$$D = Md/(Md - Mi) \times Dw$$

Where Md, Mi, and Dw are dry mass, immersed mass and density of water, respectively.

2.2.3 N_2 adsorption-desorption analysis

The pore texture of the glass particles was studied using N_2 adsorption-desorption method with an automatic nitrogen adsorption pore size analyzer (Belsorp mini II, Japan). Prior to all the analyses, the moisture was firstly removed from the samples through the degassing procedure by using a vacuum process at 150°C for 18–20 h. The nitrogen adsorption analysis provides information about the specific surface area, average pore size, and pore volume. Specifically, the specific surface area was assessed by using the Brunauer-Emmet-Teller (BET) method, and the pore size distribution (along with the mean pore size) was determined by the non-local density functional (NLDFT) theory approach [33].

2.2.4 X-ray diffraction

X-ray diffraction (XRD) was used to confirm amorphous nature of the synthesized glasses. Crystalline phases developed on the surfaces of the studied glasses after soaking in simulated body fluid (SBF) were also identified by XRD analysis. Equal amounts of each sample were analyzed by using a Philips PW 3710 apparatus equipped with a monochromatized Cu-Kα radiation (wavelength λ = 1.54056 Å) under a voltage of 40 kV and current of 30 mA. The XRD patterns were recorded in the interval $10^\circ \leq 2\theta \leq 80^\circ$ at a scan speed of 2°/min.

2.2.5 FTIR analysis

The calcinated glass powders were examined by Fourier-transform infrared spectroscopy (FTIR) by using a Nicolet NEXUS 870 FT-IR spectrometer (Thermo-Fisher, USA) before and after in vitro bioactivity tests. In the beginning, the samples were mixed with KBr at a weight ratio of 1/100 and palletized under vacuum. Subsequently, the pellets were introduced into the spectrometer, and FTIR spectra were recorded in the range of 400 to 4400 cm^{-1} with a resolution of 4 cm^{-1}.

2.2.6 Microscopic observations

The morphology and size of the glass particles were studied using transmission electron microscopy (TEM) by a Philips CM120 instruments operating at 100 kV. The glass particles were initially dispersed in ethanol (0.1 g/10 mL) followed by ultrasound treatment for 15 min. Subsequently, the samples for TEM inspection were prepared by pouring one drop of particle dispersion on a carbon-coated grid.

The surface morphology and microstructure of the glasses immersed in SBF solution was observed using a scanning electron microscope (SEM) (XL30 Philips-SEM, GER) at an accelerating voltage of 15 kV. Before being scanned, the samples were sputter-coated with a thin layer of gold (Desk sputter coater, NSC, Iran). Moreover, the chemical compositions of the samples were semi-quantitatively evaluated by a X-ray energy dispersive spectroscopy probe (EDX; Rontec, Germany) directly connected to SEM.

2.2.7 In vitro bioactivity tests

Particles of each glass composition were soaked in SBF prepared according to the Kokubo's protocol [34] using a powder-to-solution ratio of 1.5 mg/mL, as recommended by the Technical Committee 4 (TC04) of the International Commission on Glass [35]. The samples were sealed in plastic bottles and placed in a static incubator at 37°C for 7 days. At the end of the experiments, the particles were collected by filtration, washed with deionized water, left to dry overnight at room temperature, and finally investigated by SEM coupled with EDX.

3 Results

3.1 Thermal analyses

The results of TGA and DSC analyses of the synthesized glasses are presented in Figure 1. As it can be seen in the exemplary TGA graph for 58S glass, there are three main weight losses in the temperature ranges of 40-180, 180-360, and 360-570°C as a result of thermal removal of free water and alcohol (first drop), alkoxides groups (second drop), and decomposition of nitrates (third drop). The results of DSC analysis were in accordance with TGA data, showing two clear endothermic peaks for water evaporation and nitrate decomposition (at about 100-120 and 500°C, respectively) as well as an exothermic peak (centered at about 950°C), related to crystallization of the samples and the simultaneous formation of β-wollastonite ($CaSiO_3$) and cristobalite (SiO_2) crystalline phases. There was observed no significant weight loss above 700°C (calcination) confirming the successful removal of all the residuals below this temperature. Analogous results were found for F- and Ag-containing glasses with no significant differences.

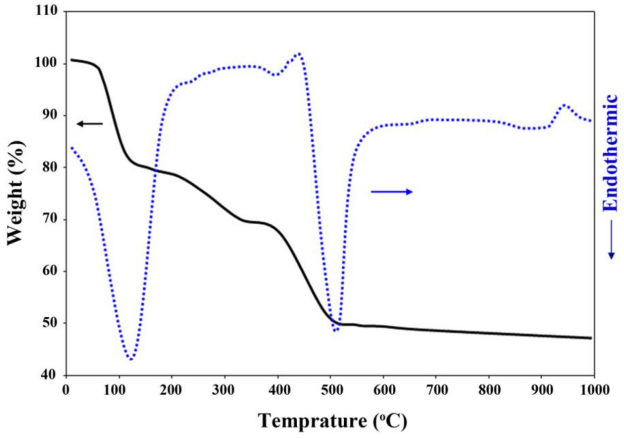

Figure 1: Example of thermal analysis curves of the synthesized glass (58S BG sample)

3.2 Densitometry

The results of densitometry of the glasses provides an early evidence of the successful incorporation of both therapeutic ions into the 58S-based structure. In fact, an increase in the density of the F- and Ag-containing glasses (2.70 and 2.72 g cm^{-3} respectively) was observed in comparison to the control group (2.67 g cm^{-3}).

3.3 Textural properties

The results obtained from the Brunauer–Emmett–Teller (BET) analysis of the synthesized glasses revealed a type IV isotherm of the Brunauer–Deming–Deming–Teller theory (BDDT) classification [36] for all the materials prepared. Table 2 collects the textural parameters of the sol-gel glass powders. From these results, it can be inferred that all the prepared glass powders have pore sizes in the mesoporous range (2-50 nm).

Table 2: Textural data of the synthesized glasses obtained by nitrogen adsorption-desorption porosimetry

Sample	Specific surface area (m^2g^{-1})	Pore volume (cm^3g^{-1})	Pore size (nm)
Control (58S glass)	136.5	0.78	14.6
$5CaF_2/0Ag_2O$	122.8	0.63	15.3
$5CaF_2/1Ag_2O$	110.1	0.58	24.1

3.4 X-ray diffraction

The XRD patterns of the prepared BGs before and after incubation in SBF are given in Figure 2A, B. By observing the patterns, it is easy to infer that all the three calcinated materials are amorphous and possess a glassy state before immersion in SBF. However, low-intensity peaks (highlighted in yellow in Figure 2A) are visible in the XRD patterns of the F- and Ag-containing samples, which might be related to the presence of CaF_2 (introduced during the synthesis process) and/or the formation of small amounts of fluorapatite during calcination. This is consistent with thermal analyses (Figure 1) showing that the onset of crystallization of calcium-silicate phases is well above the temperature used for calcination (700°C). After 7 days of immersion in SBF, the presence of diffraction peaks related to the formation of an apatite-like/fluorapatite layer was observed for all the samples.

3.5 FTIR analysis

The FTIR spectra of the BG particles after in vitro bioactivity tests confirmed the results of the XRD analysis reported in Figure 2B. The formation of an apatite-like layer on all the groups was observed after 7 days of immersion in SBF (see Figure 3). The bands centered at 450 and 1200 cm^{-1}

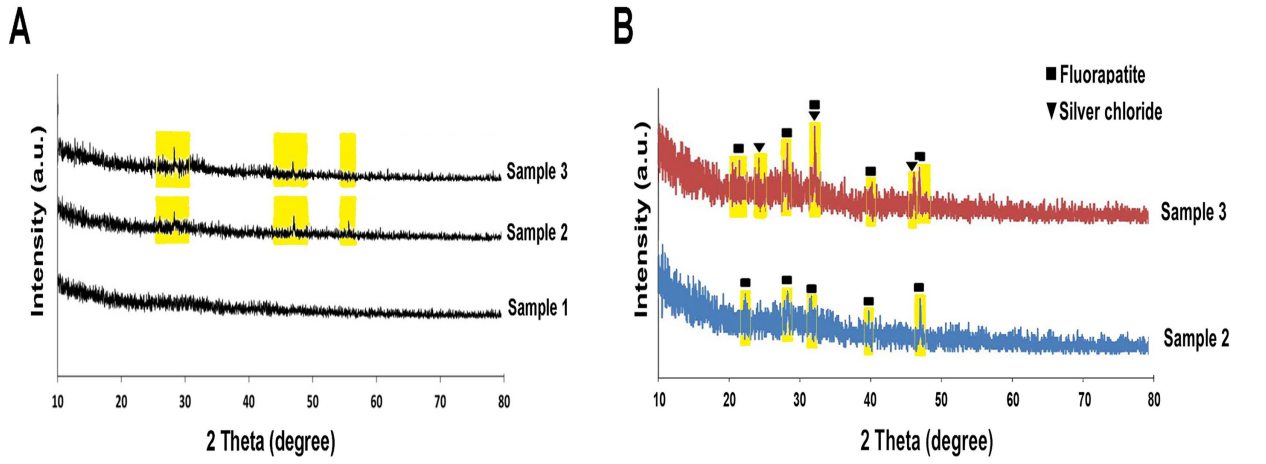

Figure 2: X-ray diffractograms of the sol-gel BGs (A) before incubation in simulated body fluid (SBF) and (B) after 7 days of incubation in SBF. Sample 1: 58S BG, sample 2: $5CaF_2/0Ag_2O$, and sample 3: $5CaF_2/1Ag_2O$

are associated with the P–O bonds in the newly-formed layer, and those at 800 and 3500 cm^{-1} can be due to hydroxyl groups [37]. The peak at 1500 cm^{-1} is related to the presence of carbonate groups in the apatite structure, confirming the formation of hydroxyl carbonate apatite crystals along with other phases such as fluorapatite and hydroxyapatite.

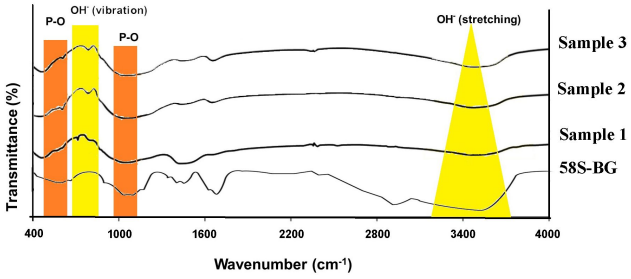

Figure 3: FTIR spectra of the 58S-BG before immersion in simulated buffer fluid (SBF) and the glasses after 7 days of immersion in SBF; Sample 1: 58S BG, sample 2: $5CaF_2/0Ag_2O$, and sample 3: $5CaF_2/1Ag_2O$

3.6 TEM observation

The TEM micrographs revealed that the glass particles are in the nano-sized scale. As shown in Figure 4, the shape of the nano-particles is quite irregular, and their size is less around 100 nm.

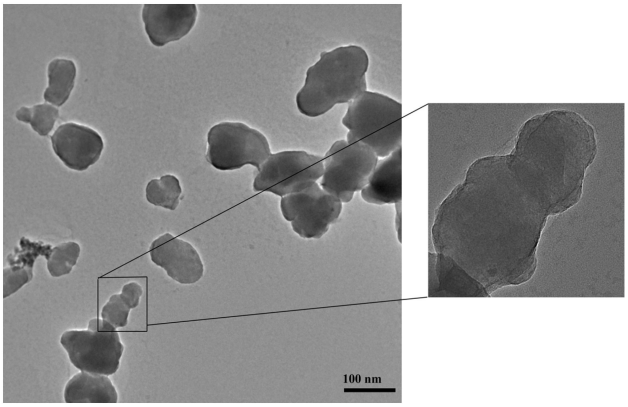

Figure 4: Transmission electron microscopy (TEM) micrographs of the prepared nano-sized 58S BGs particles

3.7 SEM observations and EDX analysis

The shape and surface morphology of the samples after incubation in SBF is shown in Figure 5. The existence of an apatite-like layer onto the BG surfaces after 7 days of soaking in SBF was confirmed for all the samples as calcium-phosphate-rich spherical agglomerates with a typical "cauliflower morphology" are well visible.

The data obtained from EDX analysis suggests that the high peaks of Ca and P can be attributable to this newly-formed phase; the peak of Si is due to the presence of the glass nanoparticles lying underneath. Compositional analysis also revealed the presence of Ag and F after incubation in SBF. It should be noted that the peak of gold (Au) on the glasses surfaces was only associated with the coating gold layer before the SEM imaging.

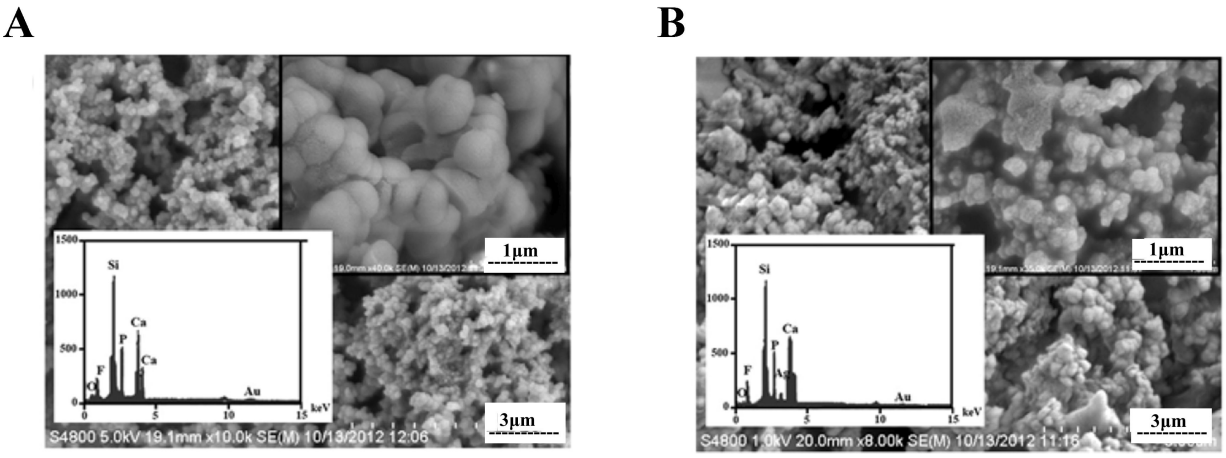

Figure 5: SEM micrographs of (A) the $5CaF_2/0Ag_2O$ group and (B) the $5CaF_2/1Ag_2O$ group at 7 days post-incubation in SBF. The relevant EDX spectra of both samples are given, confirming the presence of therapeutic ions

4 Discussion

Up to now, different types of biomedical glasses have been developed and applied in bone repair and regeneration strategies [11]. However, more research is needed to achieve an optimized composition covering all therapeutic aspects around bone healing processes, like improving osteogenesis and avoiding bacterial infections. In this regard, a number of therapeutic ions have been added to the basic structure of glasses including strontium, zinc, gallium, and so on [38]. In this study, we successfully synthesized a series of 58S-based BGs containing fluoride and silver ions with the aim of covering both the above-mentioned issues, *i.e.* simultaneously improving bone regeneration and controlling antibacterial infections. It has been previously proven that fluoride ions (F^-) can stimulate bone formation and prevent osteoporosis-related fractures [39]. Also, the antibacterial effects of silver ions (Ag^+) have been widely documented in the literature [40]. When incorporated into the glass structure, silver can prevent bacterial growth and reproduction in vivo [41]. Although adding these two ions to melt-derived biomedical glasses has been previously evaluated [42], there is a relative paucity of studies on the incorporation of F and Ag in sol-gel glasses. Specifically, the present study provides new information on the simultaneous incorporation of both ions into the 58S BG composition.

DTA and TGA analyses (Figure 1) revealed that the temperature of 700°C is enough to remove all the organic residuals and to stabilize all the glass powders. Similar to previously reported studies on glasses [20], the TGA graph exhibits a distinct step between 40-180°C due to the weight loss of physically adsorbed water. The second step is around 180-360°C, which is related to the decomposition of alkoxides groups, followed by the third step (400-500°C), which is associated with nitrate decomposition.

Determined by the Archimedes method, the density of the samples provides a preliminary evidence of the successful incorporation of F^- and Ag^+ ions into the glass structure. Specifically, the Ag-containing glass ($5CaF_2/1Ag_2O$ group) has a slightly higher density compared to the other groups. These results were in accordance with previously published studies, reporting that silver possesses higher density in comparison to fluorine [43].

Similar to other sol-gel-based glasses, the prepared samples showed a porous structure at the meso-scale confirmed by the BET analysis (see Table 2). As reported elsewhere [44], the shape of the hysteresis loop is closely related to the shape of mesopores; specifically, all the produced BGs exhibits a H2 hysteresis loop, corresponding to mesopores with undefined shape. The specific surface area of all glasses is comparable to those of 58S silicate sol-gel materials reported in the literature [45]. However, adding F^- and Ag^+ ions to the 58S composition resulted in reduced specific surface area and pore volume. As previously reported, F^- ions through creating a dense and interconnected network reduce the pore volume in the sol-gel BGs [46]. It has also been reported that Ag^+ ions can precipitate in the glass network during the hydrolysis and condensation processes and, thereby, block the formation of glass mesopores [47].

The XRD patterns of all glasses revealed their amorphous structure before immersion in SBF (see Figure 2A). However, the formation of an apatite-like layer was observed after 7 days of incubation in SBF. As shown in Figure 2B, the peaks related to fluorapatite and silver chloride are obviously seen in the $5CaF_2/0Ag_2O$ and $5CaF_2/1Ag_2O$

groups, respectively. These peaks confirmed the successful incorporation of both ions into the different glass samples. Silver, which was present as a modifier in the glass network, was released in the form of Ag^+ ions that, after combining with Cl^- ions from the solution, formed AgCl. The results of FTIR spectroscopy was in agreement with the XRD data, confirming the formation an apatite-like layer on the glass surfaces after 7 days of immersion in SBF (Figure 3). The peaks near the wavelengths of 465 and 1078 cm^{-1} are possibly related to the vibrational modes of P-O bonds of apatite/ fluorapatite [48, 49]. Furthermore, the displacement of the OH^- peaks between 800 and 3500 cm^{-1} is an additional evidence of the formation of a fluorapatite layer.

TEM observation showed that the size of the 58S-based glass particles is smaller than 100 nm (Figure 4). This size shows that the applied synthesis technique is appropriate for providing nano-sized glass particles. The SEM micrographs of all the SBF-immersed glasses showed that an apatite-like layer forms on them. These data are in line with ISO 23317 (Implants for surgery), declaring that the glass must be bioactive before 4 weeks post-immersion in SBF solution [50]. The peaks of F^- and Ag^+ ions are obviously seen in the EDX spectra of the substituted glasses, confirming the presence of these two ions in the samples.

5 Conclusions

In brief, the authors could successfully synthesize a series of F- and Ag-substituted glasses based on the 58S sol-gel BG composition. The analyses of DSC, XRD, FTIR, TEM, and SEM were conducted to reveal the physico-chemical characteristics of the synthesized samples. All these 58S-derived nano-sized materials were predominantly amorphous after calcination and exhibit bioactvie properties after immersion in SBF. N_2 adsorption-desorption results clarified the mesoporous structure of all the sol-gel prepared glasses. Considering their apatite-forming ability, which is the key to osteointegration, and antibacterial activities (shown in a previously published report), these co-doped glasses show promise for use in bone/dental tissue reconstruction and deserve to be further investigated to better clarify the structure-property-function relationships in the context of targeted clinical applications.

Ethical approval: The conducted research is not related to either human or animals use.

Conflict of Interests: The authors declare no conflict of interest regarding the publication of this paper.

References

[1] Rahaman M.N., Day D.E., Sonny Bal B., Fu Q., Jung S.B., Bonewald L.F., Tomsia A.P., Bioactive glass in tissue engineering, Acta Biomater., 2011, 7(6), 2355-2373.

[2] Kargozar S., Mozafari M., Hashemian S.J., Brouki Milan P., Hamzehlou S., Soleimani M., Joghataei M.T., Gholipourmalekabadi M., Korourian A., Mousavizadeh K., Osteogenic potential of stem cells-seeded bioactive nanocomposite scaffolds: A comparative study between human mesenchymal stem cells derived from bone, umbilical cord Wharton's jelly, and adipose tissue. Journal of Biomedical Materials Research Part B: Applied Biomaterials 2018, 106:61-72.

[3] Johari B., Kadivar M., Lak S., Gholipourmalekabadi M., Urbanska A.M., Mozafari M., Ahmadzadehzarajabad M., Azarnezhad A., Afshari S., Zargan J., Osteoblast–seeded bioglass/gelatin nanocomposite: a promising bone substitute in critical-size calvarial defect repair in rat, Int. J. Artif. Organs, 2016, 39, 524-33.

[4] Kargozar S., Mozafari M., Hamzehlou S., Brouki Milan P., Kim H.-W., Baino F., Bone tissue engineering using human cells: a comprehensive review on recent trends, current prospects, and recommendations, Appl. Sci., 2019, 9, 174.

[5] Campana V., Milano G., Pagano E., Barba M., Cicione C., Salonna G., Lattanzi W., Logroscino G., Bone substitutes in orthopaedic surgery: from basic science to clinical practice, J. Mater. Sci. Mater. Med. 2014, 25, 2445-2461.

[6] Kargozar S., Lotfibakhshaiesh N., Ai J., Mozafari M., Milan P.B., Hamzehlou S., Barati M., Baino F., Hill R.G., Joghataei M.T., Strontium-and cobalt-substituted bioactive glasses seeded with human umbilical cord perivascular cells to promote bone regeneration via enhanced osteogenic and angiogenic activities, Acta Biomater., 2017, 58, 502-514.

[7] Kargozar S., Baino F., Hamzehlou S., Hill R.G., Mozafari M., Bioactive glasses: sprouting angiogenesis in tissue engineering, Trends Biotechnol., 2018, 36, 430-444.

[8] Kargozar S., Baino F., Hamzehlou S., Hill R.G., Mozafari M., Bioactive glasses entering the mainstream, Drug Discov. Today, 2018, 23, 1700-1704.

[9] Miola M., Pakzad Y., Banijamali S., Kargozar S., Vitale-Brovarone C., Yazdanpanah A., Bretcanu O., Ramedani A., Verne E., Mozafari M., Glass-ceramics for cancer treatment: so close, or yet so far? Acta Biomater., 2019, 83, 55-70.

[10] Mozafari M., Banijamali S., Baino F., Kargozar S., Hill R.G. Calcium carbonate: Adored and ignored in bioactivity assessment, Acta Biomater., 2019, 91, 35-47.

[11] Baino F., Hamzehlou S., Kargozar S. Bioactive glasses: where are we and where are we going?, J. Funct. Biomater. 2018, 9, 25.

[12] Kargozar S., Mozafari M., Hamzehlou S., Baino F., Using Bioactive Glasses in the Management of Burns, Front. Bioeng. Biotechnol., 2019, 7, 62.

[13] Kargozar S., Hamzehlou S., Baino F., Can bioactive glasses be useful to accelerate the healing of epithelial tissues?, Mater. Sci. Eng. C, 2019, 97, 1009-1020.

[14] Hench L.L., Splinter R.J., Allen W., Greenlee T., Bonding mechanisms at the interface of ceramic prosthetic materials, J. Biomed. Mater. Res. 1971, 5, 117-141.

[15] Kargozar S., Hamzehlou S., Baino F., Potential of bioactive glasses for cardiac and pulmonary tissue engineering, Materials, 2017, 10, 1429.

[16] Baino F., Fiume E., Barberi J., Kargozar S., Marchi J., Massera J., Verné E., Processing methods for making porous bioactive glass-based scaffolds - A state-of-the-art review, Int. J. Appl. Ceram. Technol., 2019, 16(5), 1762-1796.
[17] Kargozar S., Montazerian M., Fiume E., Baino F. Multiple and promising applications of Sr-containing bioactive glasses in bone tissue engineering, Front. Bioeng. Biotechnol., 2019, 7, 161.
[18] Zheng K., Boccaccini A.R., Sol-gel processing of bioactive glass nanoparticles: A review, Adv. Colloid Interface Sci., 2017, 249, 363-73.
[19] Kargozar S., Mozafari M., Hamzehlou S., Kim H.-W., Baino F., Mesoporous bioactive glasses (MBGs) in cancer therapy: Full of hope and promise, Mater. Lett., 2019, 251, 241-246.
[20] Zhu H., Hu C., Zhang F., Feng X., Li J., Liu T., Chen J., Zhang J., Preparation and antibacterial property of silver-containing mesoporous 58S bioactive glass, Mater. Sci. Eng. C, 2014, 42, 22-30.
[21] Shah F.A., Brauer D.S., Desai N., Hill R.G., Hing K.A., Fluoride-containing bioactive glasses and Bioglass® 45S5 form apatite in low pH cell culture medium, Mater. Lett., 2014, 119, 96-99.
[22] Liu J., Rawlinson S.C., Hill R.G., Fortune F., Strontium-substituted bioactive glasses in vitro osteogenic and antibacterial effects, Dent. Mater., 2016, 32, 412-422.
[23] Kargozar S., Lotfibakhshaiesh N., Ai J., Samadikuchaksaraie A., Hill R.G., Shah P.A., Milan P.B., Mozafari M., Fathi M., Joghataei M.T., Synthesis, physico-chemical and biological characterization of strontium and cobalt substituted bioactive glasses for bone tissue engineering, J. Non-Cryst. Solids, 2016, 449, 133-140.
[24] Hoppe A., Güldal N.S., Boccaccini A.R., A review of the biological response to ionic dissolution products from bioactive glasses and glass-ceramics, Biomater., 2011, 32, 2757-2774.
[25] Brauer D.S., Karpukhina N., Law R.V., Hill R.G., Structure of fluoride-containing bioactive glasses, J. Mater. Chem., 2009, 19, 5629-5636.
[26] Everett E., Fluoride's effects on the formation of teeth and bones, and the influence of genetics, J. Dent. Res., 2011, 90, 552-560.
[27] Brauer D.S., Karpukhina N., O'Donnell M.D., Law R.V., Hill R.G., Fluoride-containing bioactive glasses: effect of glass design and structure on degradation, pH and apatite formation in simulated body fluid, Acta Biomater., 2010, 6, 3275-3282.
[28] Galarraga-Vinueza M., Passoni B., Benfatti C., Mesquita-Guimarães J., Henriques B., Magini R., Fredel M., Meerbeek B., Teughels W., Souza J., Inhibition of multi-species oral biofilm by bromide doped bioactive glass, J. Biomed. Mater. Res. Part A, 2017, 105, 1994-2003.
[29] Raucci M.G., Adesanya K., Di Silvio L., Catauro M., Ambrosio L., The biocompatibility of silver-containing $Na_2O{\cdot}CaO{\cdot}2SiO_2$ glass prepared by sol–gel method: In vitro studies, J. Biomed. Mater. Res. Part B: Appl. Biomater., 2010, 92, 102-110.
[30] Wu C., Zhou Y., Xu M., Han P., Chen L., Chang J., Xiao Y., Copper-containing mesoporous bioactive glass scaffolds with multifunctional properties of angiogenesis capacity, osteostimulation and antibacterial activity, Biomaterials, 2013, 34, 422-433.
[31] Aydin Sevinç B., Hanley L., Antibacterial activity of dental composites containing zinc oxide nanoparticles, J. Biomed. Mater. Res. Part B: Appl. Biomater., 2010, 94, 22-31.
[32] Gholipourmalekabadi M., Sameni M., Hashemi A., Zamani F., Rostami A., Mozafari M., Silver-and fluoride-containing mesoporous bioactive glasses versus commonly used antibiotics: Activity against multidrug-resistant bacterial strains isolated from patients with burns, Burns, 2016, 42, 131-140.
[33] Landers J., Gor G.Y., Neimark A.V., Density functional theory methods for characterization of porous materials, Colloids Surf. Physicochem. Eng. Aspects, 2013, 437, 3-32.
[34] Kokubo T., Takadama H., How useful is SBF in predicting in vivo bone bioactivity? Biomater., 2006, 27, 2907-2915.
[35] Macon A.L., Kim T.B., Valliant E.M., Goetschius K., Brow R.K., Day D.E., Hoppe A., Boccaccini A.R., Kim I.Y., Ohtsuki C., A unified in vitro evaluation for apatite-forming ability of bioactive glasses and their variants, J. Mater. Sci. Mater. Med., 2015, 26, 115.
[36] Rouquerol J., Rouquerol F., Llewellyn P., Maurin G., Sing K.S., Adsorption by powders and porous solids: principles, methodology and applications, 2013, Elsevier.
[37] Peitl O., Zanotto E.D., Hench L.L., Highly bioactive P2O5–Na2O–CaO–SiO2 glass-ceramics, J. Non-Cryst. Solids, 2001, 292, 115-126.
[38] Baino F., Fiorilli S., Vitale-Brovarone C., Bioactive glass-based materials with hierarchical porosity for medical applications: review of recent advances, Acta Biomater., 2016, 42, 18-32.
[39] Gentleman E., Stevens M.M., Hill R.G., Brauer D.S., Surface properties and ion release from fluoride-containing bioactive glasses promote osteoblast differentiation and mineralization in vitro, Acta Biomater., 2013, 9, 5771-5779.
[40] Maillard J.-Y., Hartemann P., Silver as an antimicrobial: facts and gaps in knowledge, Crit. Rev. Microbiol., 2013, 39, 373-383.
[41] Kędziora A., Speruda M., Krzyżewska E., Rybka J., Łukowiak A., Bugla-Płoskońska G., Similarities and differences between silver ions and silver in nanoforms as antibacterial agents, Int. J. Mol. Sci., 2018, 19, 444.
[42] Balagna C., Vitale-Brovarone C., Miola M., Verne E., Canuto R.A., Saracino S., Muzio G., Fucale G., Maina G., Biocompatibility and antibacterial effect of silver doped 3D-glass-ceramic scaffolds for bone grafting, J. Biomater. Appl., 2011, 25, 595-617.
[43] Turkoz M., Atilla A.O., Evis Z., Silver and fluoride doped hydroxyapatites: investigation by microstructure, mechanical and antibacterial properties, Ceram. Int., 2013, 39, 8925-8931.
[44] Sing K., Reporting physisorption data for gas/solid systems with special reference to the determination of surface area and porosity (Provisional), Pure Appl. Chem., 1982, 54, 2201-2218.
[45] Sepulveda P., Jones J.R., Hench L.L. Characterization of melt-derived 45S5 and sol-gel–derived 58S bioactive glasses, J. Biomed. Mater. Res., 2001, 58, 734-740.
[46] Li H., Wang D., Hu J., Chen C., Crystallization, mechanical properties and in vitro bioactivity of sol–gel derived Na 2 O–CaO–SiO 2–P 2 O 5 glass–ceramics by partial substitution of CaF 2 for CaO, J. Sol-Gel Sci. Technol., 2013, 67, 56-65.
[47] Garnica-Romo M., González-Hernández J., Hernández-Landaverde M., Vorobiev Y., Ruiz F., Martínez J., Structure of heat-treated sol-gel SiO2 glasses containing silver, J. Mater. Res., 2001, 16, 2007-2012.
[48] Li P., Ohtsuki C., Kokubo T., Nakanishi K., Soga N., Nakamura T., Yamamuro T., Apatite formation induced by silica gel in a simulated body fluid, J. Am. Ceram. Soc., 1992, 75, 2094-2097.
[49] Pereira M.d.M., Clark A., Hench L., Calcium phosphate formation on sol-gel-derived bioactive glasses in vitro, J. Biomed. Mater. Res., 1994, 28, 693-698.
[50] Standard M.J., Implants for Surgery: In Vitro Evaluation for Apatite-Forming Ability of Implant Materials (ISO 23317:2007, IDT), 2010, Jabatan Standards Malaysia.